

Stopping powers of Ag and Au for 0.3–2.0-MeV ^4He ions

A. Fontell and M. Luomajärvi

Department of Physics, University of Helsinki, Helsinki, Finland

(Received 28 April 1978)

The stopping powers of Ag and Au for ^4He ions have been measured in the energy region from 0.3 to 2.0 MeV with accuracy (standard deviation) $\pm 1\%$. The energy losses of He ions were determined from the backscattering spectra. The target films were vapor-deposited on silicon wafers and the areal densities were absolutely determined by weighing. The present results are for both elements above 500 keV within 2% of the best-fit values in a recent compilation by Ziegler. The agreement is worse below 500 keV where the present results lie consistently above the best-fit values.

I. INTRODUCTION

In the past, growing interest has been displayed in the stopping processes of atomic projectiles. The widespread use of helium ions in micro-analysis has often directed interest to this projectile at energies around 1 MeV. Stopping power can be measured either absolutely or relative to another material with well-established stopping-power values. In the latter case one usually assumes that the theoretical scattering cross section is valid. As a general observation, one can say that the variously reported experimental stopping powers differ from each other more than the stated accuracies would allow. Unexpectedly large discrepancies are also often in evidence as regards the shapes of the stopping-power curves as a function of the helium-ion energy.

There are numerous reasons for the large scatter in the experimental results in the region of 1 MeV, where the helium stopping goes through a maximum and where no stopping theory exists. If an absolute thin-film measurement is considered, the demands on the film purity, homogeneity, and accuracy in the areal density are very high. If, on the other hand, a relative measurement is considered, one has to pay attention to, e.g., possible changes in the scattering law as the bombarding energy is changed. Regarding especially the shape of the stopping-power curve, the energy calibration of the accelerator, and the determination of the detector energy response in the whole energy region used are essential. An additional uncertainty in the results is often caused by texture in the targets.

In this work, in which thin films with absolutely determined areal densities are used, special attention is paid to reducing all the above-mentioned error sources. Ag and Au, which are two of the most extensively studied elements, have been chosen as the objects of these measurements. In the case of Au the previous results¹⁻¹⁴ are surprisingly widely scattered and the only way to get

well-established values would seem to be to repeat the measurements carefully in different laboratories. The agreement in the case of Ag is somewhat better.¹⁰⁻¹⁷ The choice of these elements is motivated by the fact that in many kinds of measurements certain stopping-power standards are urgently needed. The elements selected for these standards should cover a broad region in atomic numbers, be chemically stable, and be easy to deposit by vacuum evaporation. It is for this reason that the experimental interest has so often been directed towards such elements as Al, Cu, Ag, and Au. A recent publication¹⁸ collects the experimental stopping data and gives a clear picture of the abundance and the scatter of results for all elements.

II. EXPERIMENTAL METHOD

A. Bombarding and detecting conditions

The targets were thin films of Ag or Au on silicon wafers. A silicon surface-barrier detector was used in recording the backscattering spectra, and the stopping powers were calculated from the energy differences between the ions scattered from the front and back surfaces of the films.

The $^4\text{He}^+$ ions obtained from the Van de Graaff accelerator of our laboratory, were deflected 90° along a path with a radius of 0.6 m in an energy-analyzing magnet. The energy resolution [full width at half-maximum (FWHM)] of the resulting beam was better than 1 keV. During every run, the magnet was calibrated by means of the $^{13}\text{C}(p, \gamma)^{14}\text{N}$ and $^{20}\text{Ne}(\alpha, \gamma)^{24}\text{Mg}$ resonance reactions at¹⁹ $E_p = 1747.6 \pm 0.9$ keV and $^{20}E_\alpha = 1929 \pm 5$ keV, respectively; the proton energy corresponds to a $^4\text{He}^+$ ion energy of 440.0 keV. These two reactions gave the same value to the energy calibration constant with an accuracy of $\pm 0.3\%$. In all the measurements, a standard procedure to reach the desired magnetic field was used.

The target was placed in the center of a 0.6-m-

diameter scattering chamber, which was ion pumped to a vacuum of about 5×10^{-5} Pa. The ion beam (of the order of nA) was collimated to an area of about 0.5 mm^2 . A fresh target area was usually moved into the beam for every spectrum. During the measurements either an annular detector, mounted coaxially with the beam, or an ordinary shaped detector at a scattering angle of 170° was used. In the former case the target surface was perpendicular to the beam and in the latter case it was tilted through 5° in the direction of the detector. In the latter case the target was also rotated during the entire measurement to avoid possible channelling effects. The energy resolution (FWHM) of the detecting system was 15 keV.

The energy response of a silicon surface-barrier detector is affected by the surface dead layer and by the elastic energy loss in the detector.²¹ One result of these effects is that the particle energy per channel is not constant. During every run the dependence of this quantity on the He ion energy was determined by observing the shifts in the leading edges when the energy was changed or when targets with different mass numbers were bombarded. In this way, the particle energy per channel was determined from energy shifts that were comparable to the energy losses in the films. Figure 1 illustrates the results obtained during one such run. It can be seen that at the low-energy end this correction affects the stopping-power values by up to 2%–3%.

B. Target preparation

The targets were prepared by vacuum evaporation in an ultrahigh-vacuum chamber under a vacuum of 10^{-5} Pa. The material purity was better than 99.9%. Polished silicon wafers, many of which were also oxidized, were used as backing plates. The wafer was fixed onto a water-cooled holder situated 26 cm above a resistance heated tungsten boat. A circular mask determined the area of the deposit. For Ag and Au masks of area 7.03 and 5.96 cm^2 , respectively, were used.

To determine the areal densities of the targets the wafers were weighed with a microbalance (Mettler M5) before and after the vapor deposition. The areal densities varied between 84 and $230 \mu\text{g}/\text{cm}^2$. The homogeneity of the deposits was checked by measuring the spectra from many places in the samples.

C. Data collection and analysis

The measurements were usually started at an energy of 2.0 MeV and were continued to lower energies in steps of 200 keV or smaller. At

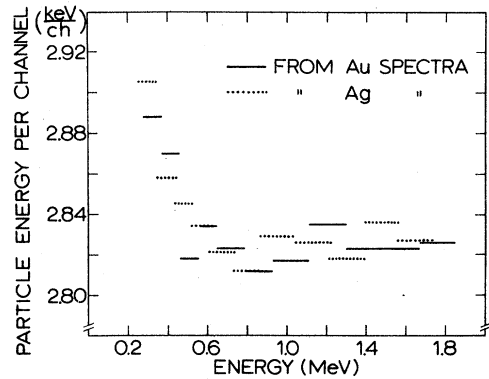


FIG. 1. Particle energy per channel as a function of ^4He ion energy. The values were determined from the shifts in the leading edges when the energy was changed. The bar lengths give the magnitudes of the energy shifts.

each energy, two spectra were recorded from every film used. The channel width was adjusted to about $2.8 \text{ keV}/\text{channel}$ and the measurements were continued until an intensity of about 4000 counts/channel was reached at the high-energy edges of the spectra. The channels corresponding to the scattering from the front and back surfaces of the films were determined from the half-height points. By using the experimentally determined values for particle energy per channel, the energy losses in the films were obtained.

The stopping powers were calculated from the equation derived in the linear approximation²²

$$S(\bar{E}_{in}) = \frac{\Delta E}{\rho \Delta t [K / \cos \theta_1 + S(\bar{E}_{out}) / S(\bar{E}_{in}) \cos \theta_2]},$$

where \bar{E}_{in} and \bar{E}_{out} are the average incoming and outgoing energies in the film, ΔE is the observed energy loss, $\rho \Delta t$ is the areal density of the film, K is the kinematic factor,⁸ and θ_1 and θ_2 are the angles between the target normal and the trajectories of the incident and scattered ions, respectively. An iterative procedure was employed where as starting values \bar{E}_{in} and \bar{E}_{out} were obtained from an approximative formula²² and the earlier published values were used for the stopping-power ratio $S(\bar{E}_{out})/S(\bar{E}_{in})$. For both elements four iterations resulted in stable stopping-power values.

III. RESULTS AND DISCUSSION

The stopping-power results are presented in Fig. 2, where the areal densities of the films are also given. Every point is the mean value of the two measurements performed in each case. No systematic difference can be noticed between the Au points measured by using rotating or non-rotating targets. We conclude that channelling did

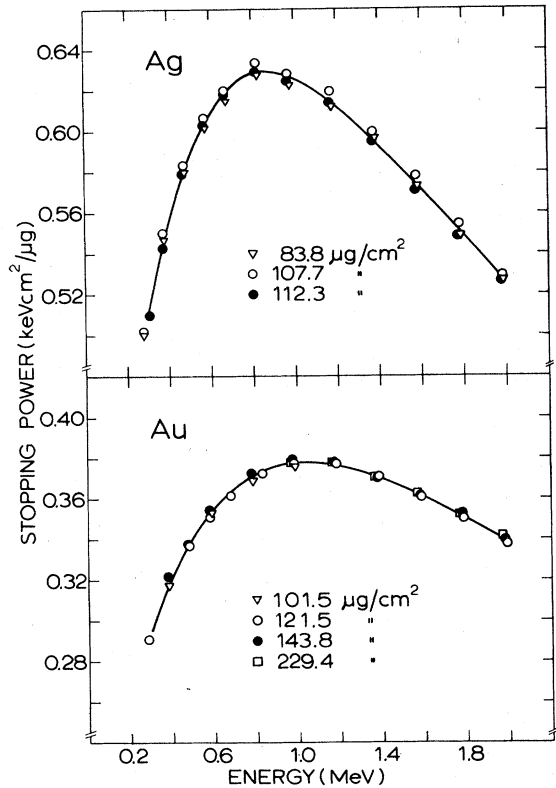


FIG. 2. Stopping powers of Ag and Au for ^4He ions. The solid line is a polynomial fit to the experimental points. For all the Ag films and for the $121.5\text{-}\mu\text{g}/\text{cm}^2$ Au film the rotating target technique was employed.

TABLE I. Stopping powers of Ag and Au for ^4He ions.

E^a (keV)	Stopping power (keV cm ² /μg)	
	Ag ^b	Au ^b
300	0.511	0.295
400	0.555	0.321
500	0.587	0.340
600	0.608	0.355
700	0.622	0.365
800	0.628	0.372
900	0.629	0.376
1000	0.626	0.378
1100	0.620	0.377
1200	0.612	0.376
1300	0.603	0.373
1400	0.593	0.370
1500	0.582	0.366
1600	0.571	0.361
1700	0.560	0.356
1800	0.549	0.350
1900	0.537	0.344
2000	0.525	0.338

^a Estimated standard deviation $\pm 0.3\%$.

^b Estimated standard deviation $\pm 1\%$, except at the lowest energy, where it is 1.5% .

not affect the energy-loss values. A Brice formula²³ fit to our experimental points was calculated. The following values for the three adjustable parameters were obtained: $Z = 2.290$ (3.430), $a = 0.3550$ (0.3107), and $n = 3.097$ (2.953) in the case of Ag (Au). The fitting had a standard deviation of about 1% for both elements. Polynomial fits, also, were tried. A fourth-power polynomial with the coefficients $a_0 = 0.2868$ (0.1832), $a_1 = 1.035$ (0.5006), $a_2 = -1.077$ (-0.4502), $a_3 = 0.4540$ (0.1687), and $a_4 = -0.07229$ (-0.02466) for Ag (Au) was selected. The standard deviation in the polynomial fitting was about 0.6% for both elements. Due to the somewhat smaller standard deviation, the polynomial fits were used in the interpolations and the values at the extreme energies were estimated straight from the experimental points. The stopping-power values obtained in this way are listed in Table I.

The accuracy of the stopping-power results is determined mainly by the errors in the measurements of the film thicknesses and the energy losses. The accuracy of the film-area determination was better than $\pm 0.01\text{ cm}^2$ and that of the weighing $\pm 2\text{ }\mu\text{g}$. Including inhomogeneity, the standard deviation in the areal density is estimated to be

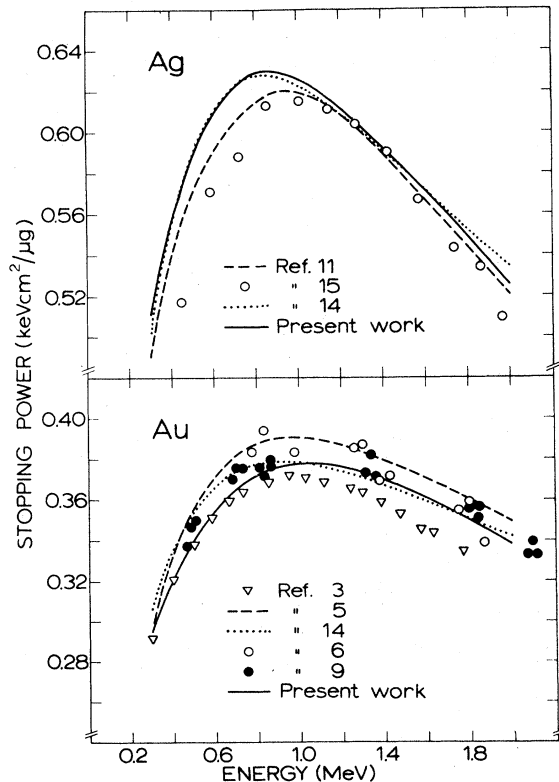


FIG. 3. Comparison of the measured stopping powers with earlier absolute measurements.

$\pm 0.5\%$ for the thickest and $\pm 0.8\%$ for thinnest film used. The measurements indicated that the channel difference corresponding to the energy loss could be determined with an accuracy of ± 0.2 channels. When the uncertainty in the particle energy per channel ($\pm 0.4\%$) is added to this, a standard deviation from $\pm 0.6\%$ to $\pm 1.0\%$ is obtained. The lower limit is for the largest energy loss and the higher for the smallest. The error caused by the use of the linear approximation in the calculations is less than $\pm 0.1\%$. When a quadratic combination of these errors is assumed, a standard deviation from $\pm 0.8\%$ to $\pm 1.3\%$ in the stopping-power values is obtained. The accuracy in the final results is taken to be $\pm 1\%$ except at the lowest energy where it is somewhat poorer. The present results are compared to earlier absolute measurements in Fig. 3. (For more complete tabulation of earlier results see Ref. 18.) In the case of Ag our results are in very good agreement with those of Ref. 14. There is a rather big difference in the form of the stopping-power curve

as between our results and those of Refs. 11 and 15, although the results coincide at around 1.4 MeV. The results in Ref. 16 come much closer to the present values, if the aluminum stopping power used as a reference is taken from Ref. 24 instead of from Ref. 15. Above 700 keV the difference between the present values and the best-fit values in Ref. 18 is less than 1.2%; at 300 keV our value is 5.4% above the best-fit value in Ref. 18.

In the case of Au our results coincide with those of Ref. 3 at the low energies and with those of Ref. 14 at the high energies. The results of Ref. 7, not shown in Fig. 3, lie consistently below our values and those of Ref. 9 follow very nicely the form of our curve but lie consistently about 1% higher. Above 500 keV the best-fit values in Ref. 18 are within 1.5% of our values, but at 300 keV they are already 9% lower. It should perhaps be stressed that, if the changes in the value of the particle energy per channel are overlooked, too-low stopping powers are obtained with the thin-film method at low energies.

¹H. W. Wilcox, Phys. Rev. **74**, 1743 (1948).

²P. Ehrhart, W. Rupp, and R. Sizmann, Phys. Status Solidi **28**, K35 (1968).

³J. A. Borders, Radiat. Eff. **16**, 253 (1972).

⁴W. K. Chu, J. F. Ziegler, I. V. Mitchell, and W. D. Mackintosh, Appl. Phys. Lett. **22**, 437 (1973).

⁵W. K. Lin, H. G. Olson, and D. Powers, Phys. Rev. B **8**, 1881 (1973).

⁶J. M. Harris and M.-A. Nicolet, Phys. Rev. B **11**, 1013 (1975).

⁷B. M. U. Scherzer, P. Børgesen, M.-A. Nicolet, and J. W. Mayer, in *Ion Beam Surface Layer Analysis*, edited by O. Meyer, G. Linker, and F. Käppeler (Plenum, New York, 1976), p. 33.

⁸P. Børgesen and M.-A. Nicolet, Nucl. Instrum. Methods **140**, 541 (1977).

⁹S. Matteson, J. M. Harris, R. Pretorius, and M.-A. Nicolet, Nucl. Instrum. Methods **149**, 163 (1978).

¹⁰D. I. Porat and K. Ramavataram, Proc. R. Soc. A **252**, 394 (1959).

¹¹D. I. Porat and K. Ramavataram, Proc. Phys. Soc. London **78**, 1135 (1961).

¹²Ya. A. Teplova, V. S. Nikolaev, I. S. Dmitriev, and

L. N. Fateeva, Zh. Eksp. Teor. Fiz. **42**, 44 (1962) [Sov. Phys. JETP **15**, 31 (1962)].

¹³H. Nakata, Can. J. Phys. **47**, 2545 (1969).

¹⁴W. K. Lin, S. Matteson, and D. Powers, Phys. Rev. B **10**, 3746 (1974).

¹⁵W. K. Chu and D. Powers, Phys. Rev. **187**, 478 (1969).

¹⁶E. Leminen and A. Fontell, Radiat. Eff. **22**, 39 (1974).

¹⁷G. E. Hoffman and D. Powers, Phys. Rev. A **13**, 2042 (1976).

¹⁸J. F. Ziegler, *Helium: Stopping Powers and Ranges in All Elemental Matter* (Pergamon, New York, 1977).

¹⁹F. Ajzenberg-Selove, Nucl. Phys. A **268**, 1 (1976).

²⁰P. J. M. Smulders, Physica (Utr.) **31**, 973 (1965).

²¹J. B. Mitchell, S. Agami, and J. A. Davies, Radiat. Eff. **28**, 133 (1976).

²²W. K. Chu, in *New Uses of Ion Accelerators*, edited by J. F. Ziegler (Plenum, New York, 1975), p. 142.

²³D. K. Brice, Phys. Rev. A **6**, 1791 (1972).

²⁴M. Luomajärvi, A. Fontell, and M. Bister, in *Ion Beam Surface Layer Analysis*, edited by O. Meyer, G. Linker, and F. Käppeler (Plenum, New York, 1976), p. 75.